Published in final edited form as:
J Bone Miner Res. 2012 January ; 27(1): 79–92. doi:10.1002/jbmr.531.

Regulation of Human Osteoclast Development by Dendritic Cell-Specific Transmembrane Protein (DC-STAMP)

Ya-Hui Chiu[1,2,*], **Kofi A. Mensah**[2,3], **Edward M. Schwarz**[2,3], **Yawen Ju**[2,4], **Masahiko Takahata**[2,3], **Changyong Feng**[5], **Loralee A. McMahon**[4], **David G. Hicks**[4], **Ben Panepento**[1], **Peter C. Keng**[6], and **Christopher T. Ritchlin**[1,2,*]

Ya-Hui Chiu: Grace_Chiu@urmc.rochester.edu; Kofi A. Mensah: Kofi_Mensah@urmc.rochester.edu; Edward M. Schwarz: Edward_Schwarz@urmc.rochester.edu; Yawen Ju: yju@urmc.rochester.edu; Masahiko Takahata: Masahiko_Takahata@urmc.rochester.edu; Changyong Feng: Feng@bst.rochester.edu; Loralee A. McMahon: Loralee_Mcmahon@urmc.rochester.edu; David G. Hicks: David_Hicks@urmc.rochester.edu; Ben Panepento: Ben_Panepento@urmc.rochester.edu; Peter C. Keng: Peter_Keng@urmc.rochester.edu; Christopher T. Ritchlin: Christopher_Ritchlin@urmc.rochester.edu

[1]Allergy/Immunology & Rheumatology Division, School of Medicine and Dentistry, University of Rochester, 601 Elmwood Ave., Rochester, NY 14642, USA

[2]The Center for Musculoskeletal Research, School of Medicine and Dentistry, University of Rochester, 601 Elmwood Ave., Rochester, NY 14642, USA

[3]Department of Microbiology and Immunology, School of Medicine and Dentistry, University of Rochester, 601 Elmwood Ave., Rochester, NY 14642, USA

[4]Department of Pathology, School of Medicine and Dentistry, University of Rochester, 601 Elmwood Ave., Rochester, NY 14642, USA

[5]Department of Biostatistics and Computational Biology, School of Medicine and Dentistry, University of Rochester, 601 Elmwood Ave., Rochester, NY 14642, USA

[6]Department of Radiation Oncology, School of Medicine and Dentistry, University of Rochester, 601 Elmwood Ave., Rochester, NY 14642, USA

Abstract

Osteoclasts (OC) are bone-resorbing, multinucleated cells that are generated via fusion of OC precursors (OCP). The frequency of OCP is elevated in patients with erosive inflammatory arthritis and metabolic bone diseases. Although many cytokines and cell surface receptors are known to participate in osteoclastogenesis, the molecular mechanisms underlying the regulation of this cellular transformation are poorly understood. Herein, we focused our studies on the dendritic cell-specific transmembrane protein (DC-STAMP), a seven-pass-transmembrane receptor-like protein known to be essential for cell-to-cell fusion during osteoclastogenesis. We identified an immunoreceptor tyrosine-based inhibitory motif (ITIM) in the cytoplasmic tail of DC-STAMP, and developed an anti-DC-STAMP monoclonal antibody 1A2 that detected DC-STAMP expression on human tumor giant cells, blocked OC formation *in vitro*, and distinguished four patterns of human PBMC with a positive correlation to OC potential. In freshly isolated monocytes, DC-STAMP^{high} cells produced a higher number of OC in culture than DC-STAMP^{low} cells and the surface expression of DC-STAMP gradually declined during osteoclastogenesis. Importantly, we showed that DC-STAMP is phosphorylated on its tyrosine residues and physically interacts with SHP-1 and CD16, an SH2-domain-containing tyrosine phosphatase and an ITAM-associated protein, respectively. Taken together, these data show that DC-STAMP is a potential

[*]Corresponding authors: Dr. Ya-Hui Chiu & Dr. Christopher T. Ritchlin, Allergy/Immunology & Rheumatology Division, Box 695, School of Medicine and Dentistry, University of Rochester, 601 Elmwood Ave., Rochester, NY 14642, Phone: 585-273-2125, FAX: 585-442-3214, Grace_chiu@urmc.rochester.edu; Christopher_Ritchlin@urmc.rochester.edu.

OCP biomarker in inflammatory arthritis. Moreover, in addition to its effect on cell fusion, DC-STAMP dynamically regulates cell signaling during osteoclastogenesis.

Keywords

DC-STAMP; osteoclast; signaling; ITIM; ITAM; SHP-1; OCP; biomarker; Ps; PsA; CD16

Introduction

Skeletal homeostasis is maintained by a highly regulated balance of continuous bone remodeling that couples new bone formation by osteoblasts (OB) with bone resorption by osteoclasts (OC).[1] OC are multinucleated polykaryons derived from the same lineage of monocytic progenitor cells as dendritic cells (DC) and macrophages. During the process of osteoclastogenesis, monocytes differentiate into OC precursors (OCP) and subsequently assume a mature multinucleated OC phenotype with bone resorption activity. Circulating OCPs are increased in a number of pathologic conditions associated with excessive bone loss including Paget's disease, multiple myeloma, and psoriatic arthritis (PsA). In PsA subjects, OCP frequency was significantly elevated and correlated with the extent of radiographic damage.[2] To date, quantification of OCP relies on cell culture techniques that are time-consuming and labor-intensive. To develop an innovative approach for OCP enumeration, we centered our studies on the identification of OCP-specific cell surface markers. Recently, we showed that CD16, the Fc-gamma III receptor, is a potential surface marker of OCP.[3] In this study, we focused our studies on another candidate molecule, the dendritic cell-specific transmembrane protein (DC-STAMP).[4]

DC-STAMP, a seven-pass transmembrane protein,[5] is required for multinucleated OC formation,[6–8] for differentiation of myeloid cells,[9] and for maintenance of immune tolerance.[10] DC-STAMP expression was rapidly up-regulated when mouse cells were cultured in the presence of OC-promoting cytokines such as receptor activator of nuclear factor-κB (NF-κB) ligand (RANKL),[4] and inhibition of murine DC-STAMP with a polyclonal antibody suppressed OC formation.[4] These observations are consistent with the phenotypes of two DC-STAMP-transgenic (Tg) models. The phenotype of DC-STAMP knockout (KO) mice is distinguished by few multinucleated TRAP+ OC and increased bone mass.[7] In contrast, overexpression of DC-STAMP in Tg mice resulted in a phenotype with accelerated cell-to-cell fusion during OCP differentiation and enhanced bone resorption.[11] The inability to identify the authentic ligand of DC-STAMP, however, has greatly hampered the understanding of the downstream molecular events triggered by this molecule.

OC differentiation from monocyte precursors is modulated by a cascade of integrated signaling that ultimately leads to OC formation.[12] Macrophage colony stimulating factor (M-CSF), RANKL and several immunoglobulin-like cell surface receptors are involved in this signaling cascade.[12] Briefly, binding of M-CSF to its receptor, c-Fms, activates OC precursor cells and induces the expression of receptor activator of nuclear factor-κB (RANK) on the cell surface. Engagement of the OCP receptor RANK by RANKL subsequently triggers the recruitment of tumor necrosis factor (TNF) receptor-associated factor 6 (TRAF6) and, at the same time, promotes the phosphorylation of the surface receptors associated with the immunoreceptor tyrosine-based activation motif (ITAM)-bearing adaptor molecules. Signals from RANK and ITAM converge to activate phospholipase Cγ (PLC-γ) and to mobilize calcium,[13] which in turn induces the transcription of various OC-specific genes through the actions of nuclear factor of activated T cells c1 (NFATc1) and other transcription factors.[13] Many recent studies address the central importance of cell surface receptors, particularly ITAM-bearing proteins, in this

signaling pathway.[13] In the absence of signals delivered by ITAM-bearing proteins, activation of RANK alone is unable to initiate the activation of OC-specific genes.[13,14] Of note, ITAM-bearing proteins usually couple with counteracting partners containing immunoreceptor tyrosine-based inhibitory motif (ITIM) to modulate both immune responses and osteoclastogenesis through a signaling network.[15–17] Although the critical importance of ITAM-bearing proteins in osteoclastogenesis is well documented,[14,18,19] data on ITIM-bearing proteins is relatively limited. To date, LILRB, PIR-B, and Ly49Q are three ITIM-bearing proteins that have been shown to regulate OC development.[20,21] Although they all have ITIM, LILRB/PIR-B and Ly49Q are considered to "negatively" and "positively" regulate osteoclastogenesis, respectively. ITIM-bearing molecules constitutively recruit the SH2 domain-containing tyrosine phosphatase 1 (SHP-1) to suppress OC development *in vitro*. The central role of ITIM-bearing proteins in the regulation of osteoclastogenesis is underscored by the phenotype of the motheaten (me^v/me^v) mice in which the activity of SHP-1 is partially lost. These mice exhibit osteoporosis due to an increased OC number and enhanced bone resorption.[22,23]

Based on the repeating transmembrane structure of DC-STAMP and its cell surface localization, we surmised that DC-STAMP also participates in the network of ITAM- and ITIM-mediated signaling. Careful screening of the DC-STAMP protein sequence led us to identify a putative ITIM on the cytoplasmic tail of DC-STAMP. The presence of an ITIM raised the possibility that the role of DC-STAMP extended beyond cell fusion to include modulation of signaling during osteoclastogenesis. To further elucidate its role in osetoclastogenesis, we generated a novel anti-DC-STAMP monoclonal antibody, and examined DC-STAMP expression in human cells. We also investigated the temporal and spatial expression of DC-STAMP during OC development *in vitro,* and analyzed its interactions with other key molecules that participate in the osteoclastogenesis signaling cascade.

Materials and Methods

Study populations

Studies were carried out with the approval of the University of Rochester Medical Center Research Subjects Review Board. PsA was diagnosed based on the Moll and Wright Criteria.[24]

Cell lines

RAW264.7 was purchased from ATCC. A fusion construct was generated in which the extracellular domain of parathyroid hormone receptor (PTHR) was fused to DC-STAMP and was transfected into RAW264.7 cells by retrovirus. TurboFectin 8.0 (OriGene) was used to transfect the Myc-DC-STAMP plasmid (OriGene, supplemental data Figure S4) into RAW264.7 cells following manufacturer's instructions.

Reagents and antibodies

RANKL and MCSF were purchased from the R&D systems. Defined Fetal Bovine Serum was obtained from Hyclone. Anti-DC-STAMP polyclonal antibody KR104 was purchased from Cosmo Bio, Japan. Anti-SHP-1 monoclonal antibody, and anti-phosphotyrosine antibody 4G10 were purchased from Cell Signaling and Millipore, respectively. All other antibodies were purchased from BD Bioscience. 7-Amino-Actinomycin D (7-AAD) was included as a vital dye to exclude dead cells. The antibody cocktail used in multicolor flow cytometry experiments included 1A2 (FITC), CD16 (PE), CD14 (APC), CD3 (Pacific Blue), CD19 (APC-Cy7) and 7-AAD. Antibodies used for supplemental data Figure S3 were composed of 1A2 (FITC), HLA-DR (PE-Texas Red), CD14 (Alexa Fluor 700), CD16

(Pacific Orange), CD15 (Pacific Blue), CD11b (APC-Cy7), CD11c (PE-Cy7), CD19 (PE), CD3 (APC), and 7-AAD. To block non-specific binding, cells were treated with 5% normal mouse sera for 15 minutes at room temperature before staining.

Production, purification and fluorochrome conjugation of monoclonal antibody 1A2

A synthetic DC-STAMP peptide ^{447}EVHLKLHGEKQGTQ^{460} (NCBI accession number Q9H295) was conjugated to KLH and was injected into mice for immunization using standard protocols. One monoclonal antibody (mAb) 1A2 was identified with specificity to DC-STAMP.[25] We used the FluoReporter FITC protein labeling kit (Molecular Probes) to conjugate FITC to 1A2.

Cell isolation and monocyte enrichment

Peripheral blood mononuclear cells (PBMC) were separated from whole blood by Ficoll gradient. Human monocytes were enriched from whole peripheral blood by the Human Monocyte Enrichment Cocktail (StemCell) following the manufacturer's instructions.

Cell staining, sorting and FACS analysis

For sterile cell sorting, PBMC prepared from Ficoll gradient were resuspended in sterile PBS (10^6 cells/ml) and incubated with 1A2-FITC for 20 min at room temperature. Cells were washed twice with PBS, resuspended in PBS (5×10^6 cells/ml) and sterile sorted with the FACS Vantage sorter (Becton Dickinson Immunocytometry Systems). The fix & perm cell permeabilization reagents (Invitrogen) were used for intracellular staining of phosphorylated PLC-γ2.

For flow cytometry analysis, cells were harvested, washed once with PBS, blocked with 5% normal mouse sera for 10 min at room temperature and stained with antibodies for 20 min. Cells were washed with PBS and fixed in 2% formaldehyde. FACS data were acquired using Canto or LSRII and analyzed using CellQuest (Becton Dickinson) or FlowJo (TreeStar) software.

OC culture and TRAP staining

Purified PBMC or monocytes were cultured in RPMI (Gibco), supplemented with 8% FBS, 2mM glutamine, 50 units/ml penicillin and 50 ug/ml streptomycin. RANKL (100 ng/ml) and M-CSF (25 ng/ml) were added to cell culture to stimulate OC generation. 1×10^5 PBMC or monocytes were cultured in one well of 96-well plates. Media were replenished every 2 days. On day 8, cells were fixed with 3% formaldehyde and stained for tartrate acid phosphatase (TRAP) (Sigma). TRAP+ cells with three or more nuclei were counted as OC. A concentration of 15 μg/ml of 1A2 was maintained in cell culture to test 1A2 inhibitory effect on OC formation. We added an IgG2a-azide free isotype control antibody (BioLegend) to monocyte and PBMC cultures.

Immunoprecipitation and western blot analysis

Human PBMC purified from Ficoll gradient was lysed using the CytoBuster Protein Extraction Reagent (Novagen). For immunoprecipitation, cell lysates were pulled down with anti-DC-STAMP 1A2 or anti-CD16 3G8 using the immunoprecipitation kit (Invitrogen). Immunoprecipitates were subject to SDS-PAGE analysis, followed by blotting using PVDF membrane. The membrane was first probed with anti-phosphotyrosine mAb 4G10 (Millipore), anti-CD16 (BD Biosciences), or anti-DC-STAMP mAb 1A2, followed by HRP-conjugated light chain specific secondary antibody (Jackson ImmunoResearch). Blots were developed with the SuperSignal West Pico or Femto chemiluminescent substrate kit

(Pierce). Signals were detected either by Kodak scientific films (Eastman Kodak) or by the Image Lab software for the ChemiDoc XRS+ system (BioRad).

Immunofluorescence and immunohistochemical staining

Monocytes were enriched with the Monocyte Enrichment Cocktail (StemCell) and were cultured on glass slides with RANKL and M-CSF for 8 days. Cells were fixed in cold methanol at −20°C for 10 minutes and washed with PBS. Cells were permeabilized and blocked with 0.1% saponin and 0.2% BSA/PBS for 15 min at room temperature. Fixed cells were then stained with rhodamine phalloidin (Molecular Probes), FITC-conjugated anti-DC-STAMP 1A2 antibody and DAPI for 2 hrs at room temperature, followed by additional wash with 0.1% saponin and 0.2% BSA/PBS for 5 min. Slides were mounted in 90% glycerol and 10% 1M Tris (pH8). Images were taken using a Zeiss phase contrast fluorescence microscope. For immunohistochemical staining (Figure 1C), PBMC were spun down and fixed in 10% NBF (Cardinal Health). The cell pellet was dislodged, placed into a histology cassette, and was then embedded into paraffin. The 4-microns paraffin section was dried at 60°C for one hour, and de-paraffinized through two changes of xylene and graded alcohols. The slides were pre-treated with Target Retrieval Solution, pH 6 (Dako, Carpinteria, CA), washed several times in Wash Buffer (Dako, Carpinteria, CA), and were incubated with 1A2 or mouse IgG2a isotype control (BD Biosciences) at 1:1500 dilution for 60 minutes at room temperature. Staining was visualized by the Flex polymer based detection kit with DAB as a chromogen (Dako, Carpinteria, CA) and counterstained with Flex Hematoxylin (Dako, Carpinteria, CA).

Statistical Analysis

The permutation test with 10^5 re-samplings was used to evaluate the inhibitory effect of 1A2 on OC formation for Figure 1D(c). The distribution of 4 DC-STAMP patterns was analyzed by the Fisher's exact test. All statistical analyses were implemented by SASR 9.1 (SAS Institute Inc., Cary, NC).

Results

DC-STAMP is an ITIM-bearing protein

We previously demonstrated that OCPs arise from the CD14+CD16+ monocyte subset in PsA.[3] Based on the fact that DC-STAMP is expressed on the cell surface and is required for OC development, we examined the surface expression of DC-STAMP on CD14+CD16- and CD14+CD16+ monocytes with a commercially available anti-DC-STAMP polyclonal antibody KR104 (Figure 1A).[4] The mean fluorescence intensity (MFI) of DC-STAMP on unstained, isotype control, CD14+CD16- and CD14+CD16+ were 317 (red line), 715 (blue line), 1747 (orange line), 2748 (green line), respectively. Both CD14+CD16- and CD14+CD16+ monocytes showed surface DC-STAMP expression but CD14+CD16+ monocytes showed a relatively higher level (1747 vs. 2748), which indicates a positive association between CD16 and DC-STAMP expression in human monocytes (Figure 1A). The expression level shown in Figure 1A is the relative intensity of DC-STAMP on CD16+ and CD16- cells.

CD16 is considered an immunoreceptor tyrosine-based activation motif (ITAM)-bearing molecule due to its association with FcRγ.[19,26] The ITAM-mediated activation signal is often coupled with a counteracting inhibitory signal delivered by the immunoreceptor tyrosine-based inhibitory motif (ITIM)-bearing receptor.[20,27–29] Based on the elevated surface expression of CD16 and DC-STAMP (Figure 1A), and a reciprocal regulation of CD16 and DC-STAMP during osteoclastogenesis in which the surface expression of CD16 increased over time,[3] whereas DC-STAMP levels steadily declined (see below in Figure

4A), we postulated that DC-STAMP may contain an ITIM motif that counteracts ITAM signaling on CD16. Therefore, we screened the protein sequence of DC-STAMP and identified a putative ITIM, $S^{407}FYPSV^{412}$, in the cytoplasmic domain of DC-STAMP.

Monoclonal antibody 1A2 with anti-DC-STAMP specificity

Based on the finding that CD16+ cells express high levels of DC-STAMP (Figure 1A) and that CD16 is an OCP surface marker in PsA patients,[3] we examined if DC-STAMP could serve as an OCP marker. To this end, we generated a monoclonal antibody (mAb) against DC-STAMP. The epitope (^{447}EVHLKLHGEKQGTQ^{460}) used to generate the antibody is conserved between mice and humans and is located on the fourth extracellular domain of DC-STAMP. We identified one clone 1A2 with reactivity to DC-STAMP from a panel of hybridomas by EIA. The binding specificity of 1A2 to murine DC-STAMP was shown by western blot in our recent publication.[25]

We confirmed the specificity of 1A2 in a DC-STAMP-transfected RAW cell line and in human protein lysates after immunoprecipitation (IP). Since the natural ligand of DC-STAMP is unknown, we established a DC-STAMP fusion construct in which the extracellular domain of parathyroid hormone receptor (PTHR) was fused to DC-STAMP to induce DC-STAMP expression. This construct was transfected into RAW264.7 cells with a retroviral vector. DC-STAMP was induced and expressed after PTH was added to culture media. Figure 1B is a western blot probed by 1A2. A prominent band with the correct molecular weight (~68 kDa, labeled by a pink asterisk in lane 3 of Figure 1B) was recognized by 1A2 in the cell lysate isolated from the PTHR-DC-STAMP transfected RAW cell line. This band was not detected in crude RAW cell lysate without the fusion construct (lane 2, Figure 1B).

To examine the specificity of 1A2 in human monocytes, we immunoprecipitated (IP) human monocyte proteins with 1A2 followed by immunoblotting with 1A2. Mouse IgG2a was used to perform IP on the same cell lysate to serve as negative control. A prominent band corresponding to the molecular weight of DC-STAMP (~53kDa) was detected in immunoprecipitates by 1A2 (labeled by a blue asterisk in lane 4 of Figure 1B), but not mouse IgG2a control (lane 5 of Figure 1B).

Next, we stained human PBMC with 1A2 to examine the expression of DC-STAMP by immunohistochemistry (IHC). A proportion of PBMC was bound by 1A2 (Figure 1C(b)), indicating the expression of DC-STAMP on these cells. Since DC-STAMP is also pivotal in the formation of giant cells,[30] we examined the expression of DC-STAMP on biopsy samples collected from human giant cell tumor of bone. The expression of DC-STAMP on multinucleated ‘osteoclast-like’ giant cells from giant cell tumor was polarized as indicated by arrows shown in Figure 1C(d). The control staining with mouse IgG2a is shown in Figure 1C(a) and 1C(c).

The specificity of 1A2 was independently examined by Millipore and is well documented in the Millipore data sheet (supplemental data Figure S2(A)). We also compared 1A2 with a previously developed polyclonal anti-DC-STAMP antibody KR104 by flow cytometry and western blotting (supplemental data Figure S2(B) and S2(C)). Our data show that KR104 and 1A2 recognize different extracellular domains of DC-STAMP. Unlike 1A2 (Lane 3 in Figure 1B), KR104 failed to recognize the PTHR-DC-STAMP fusion protein expressed in PTHR-DC-STAMP-transfected RAW cell line (data not shown). Since the 1st extracellular domain of DC-STAMP was deleted in our PTHR-DC-STAMP construct, we predict that the epitope recognized by the KR104 antibody is located on the 1st extracellular domain of DC-STAMP.

Anti-DC-STAMP antibody 1A2 blocks OC formation *in vitro*

It was previously shown that anti-DC-STAMP antibody KR104 inhibited osteoclastogenesis in a murine cell line.[4] Here, we examined whether 1A2 can also block OC formation in human monocytes. In the presence of 1A2 (15–20 μg/ml), the majority of monocytes were arrested at the TRAP-positive pre-OC stage (Figure 1D(b)). The presence of 1A2 in monocyte cultures significantly inhibited OC formation as summarized in Table 1. The average OC numbers derived from 10^6 monocytes in the absence or presence of 1A2 were 489±284 and 61±107, respectively (p=0.01). Interestingly, a higher concentration of 1A2 was required to inhibit osteoclastogenesis by PBMC compared to monocytes (Figure 1D-c, 15–20 μg/ml for monocytes whereas >100μg/ml for PBMC). Inhibition of OC formation by 1A2 was dose-dependent (Figure S1) and was not observed with the isotype control (Figure 1D).

The majority of DC-STAMP-expressing cells are monocytes

Next, we examined the expression of DC-STAMP on human PBMC by 1A2. To examine DC-STAMP expression on total PBMC, cells were stained with an antibody cocktail composed of 1A2-FITC, CD14-APC, and 7-AAD. After dead cell exclusion by 7-AAD (Figure 2A(a)), PBMC were gated into monocytes (the P2 and P3 gates in Figure 2A(b)) and lymphocytes (the P1 gate in Figure 2A(b)) based on cell size and granularity using forward (FSC) and side scatter (SSC). The corresponding DC-STAMP expression on these distinct cell populations in relation to the monocyte specific marker CD14 are shown in Figure 2A(c)-(e) and overlaid in Figure 2A(f). The IgG2a isotype staining control was used to set up the cutoff lines between DC-STAMP+ and DC-STAMP-populations in Figure 2A(c)–(e). It was clear that the monocyte populations (P2 and P3, Figure 2A(d & e)) comprised the majority of DC-STAMP-expressing cells, although some cells gated in the lymphocyte population (P1 in Figure 2A(b) and (c)) also expressed DC-STAMP (28.5% in Figure 2A(c)). In conclusion, DC-STAMP was expressed on the surface of the majority of monocytes (Figure 2A(d)–(e) & 2A(f)). A higher mean fluorescence intensity (MFI) observed on monocytes suggested DC-STAMP proteins were expressed at higher levels on monocytes than lymphocytes (compare purple/green lines to blue line in Figure 2A(f)).

To overcome the challenges of gating between lymphocytes and monocytes solely by FSC/SSC (Figure 2A(b)), we included anti-CD3 and anti-CD19 antibodies to more accurately examine DC-STAMP expression on T and B cells. The antibody cocktail is detailed in the Materials & Methods. After FSC/SSC gating and dead cell exclusion (Figure 2A(a)), CD14+, CD3+ and CD19+ cells were individually gated and the expression of DC-STAMP on these 3 populations was analyzed (Figure 2B(a), CD14+: green; CD3+: blue; CD19+: red). The results were consistent with the data shown in Figure 2A(f), indicating that monocytes are the major DC-STAMP+ cells. Interestingly, a small portion of CD3+ T cells which express DC-STAMP was identified (indicated by arrow in Figure 2B(a)). We further examined the relation between the expression of CD3 and DC-STAMP in human PBMC. As shown in Figure 2B(b), approximately 12% of total CD3+ T cells were DC-STAMP+ (Figure 2B(b)). We included six fluorescence-minus-one (FMO-FITC, FMO-PE, FMO-APC, FMO-Pacific Blue, FMO-APC-Cy7, and FMO-7AAD) staining controls in all our experiments.

Additional analyses of DC-STAMP expression on the non-T, non-B cell populations is shown in supplemental data Figure S3. The 10-color staining panel included antibodies against DC-STAMP, CD14, CD3, CD19, CD11c, CD11b, CD15, CD16, HLA-DR and 7AAD. CD14, CD3 and CD19 were used to identify monocytes, T cells, B cells, and CD11c, CD11b and HLA-DR were used for monocyte and macrophage classification,[31]respectively. Figure S3 (a)–(d) depicts the step-by-step gating strategy for

gating of the non-T, non-B population. Human PBMC were first gated by FSC/SSC (Figure S3(a)), followed by dead cell exclusion using 7-AAD (Figure S3(b)), DC-STAMP+ cells (red line in Figure S3(c)) were gated, and further dissected by the pan T-cell (CD3) and pan B-cell (CD19) markers (Figure S3(d)). CD19-CD3- (31.9%, Figure S3(d), labeled as ∞) and CD19-CD3+ (38.4%, Figure S3(d), labeled as *) were two major DC-STAMP+ cell populations. Since the expression of DC-STAMP on CD3+ cells (Figure S3(d), labeled by *) was already analyzed and shown by Figure 2B, here, we focused our analyses only on the non-T, non-B population (Figure S3(d), labeled as ∞). DC-STAMP+CD3-CD19- cells (∞ in Figure S3(d)) were further dissected into 4 quadrants based on the expression of CD14 and CD16 (Figure S3(e)). The expression of the myeloid cell markers (CD11b and CD11c; Figure S3(e), i, iii, v, vii), HLA-DR, and the granulocyte marker CD15 (Figure S3(e), ii, iv, vi, viii) on these 4 quadrants was analyzed. The expression intensities of these markers were shown by the Mean Fluorescence Intensity (MFI) (numbers in Figure S3(e), i to viii). Notably, both the DC-STAMP+CD14+CD16+ (Figure S3(e), Q2: upper right quadrant) and DC-STAMP+CD14+CD16- (Figure S3(e), Q3: lower right quadrant) subsets express very high levels of CD11b and CD11c (Figure S3(e), iii and vii), suggesting that CD14+ cells (Q2 and Q3 in Figure S3(e)) were more homogenous than the CD16 single positive (Q1 in Figure S3(e)) and CD14-CD16- double negative (Q4 in Figure S3(e)) populations. A higher expression of CD11b and CD11c on the DC-STAMP+CD3-CD19-CD14+ cells (combination of Q2 & Q3 in Figure S3(e)) suggested that these cells have a high potential to be the precursors of osteoclasts (OC), dendritic cells (DC) and macrophages.

DC-STAMP is a potential marker of OCP

We identified four major DC-STAMP expression patterns by flow cytometry in PBMC isolated from PsA subjects and healthy controls (Figure 3). DC-STAMP+ cells were low or absent in pattern I, and the highest number of DC-STAMP+ cells were present in pattern IV. Table 2 lists the criteria for classification of these patterns based on the ratio of DC-STAMP + to DC-STAMP- cells. The ratio of DC-STAMP+ to DC-STAMP- was multiplied by 100 and used as the criteria to classify patterns.

To determine whether DC-STAMP is a biomarker of OCP, we examined the association between the 4 DC-STAMP expression patterns and OCP frequency. OC culture was established on PBMC isolated from 11 HC and 21 PsA subjects. Intriguingly, HC and PsA patients showed an unequal distribution in DC-STAMP patterns (Figure 3). All HC subjects belonged to the DC-STAMP expression pattern I, whereas PsA patients were distributed in all patterns with 4, 6, 5, 6 subjects in pattern I, II, III, IV, respectively (Figure 3). A significant difference in the distribution of HC and PsA within these patterns was noted ($p=0.01$). The average OC numbers derived from DC-STAMP pattern I, II, III, and IV were 50, 98, 105, and 203, respectively (Figure 3). These results indicate an association between OCP frequency and DC-STAMP patterns, given that OC frequency increased as the DC-STAMP pattern shifted from pattern I to IV.

Human monocytes down-regulated DC-STAMP during osteoclastogenesis

The alteration of DC-STAMP surface expression during OC differentiation in human monocytes has not been characterized, so we examined the dynamics of DC-STAMP cell surface expression on monocytes during osteoclastogenesis (Figure 4A). Enriched human monocytes expressed a high level of surface DC-STAMP (purple area in Figure 4A-a; red line is isotype control). DC-STAMP surface expression was down-regulated after 1 day of exposure to RANKL+M-CSF (green line in Figure 4A-b), and continued to decline after day 2 (green lines in Figure 4A, c–e). Notably, DC-STAMP surface expression decreased dramatically after day 7 (green line in Figure 4A-e), a time point when mature OC were visualized by TRAP staining.

To confirm the results obtained with flow cytometry, we examined the cellular localization of DC-STAMP on OC via fluorescence microscopy. In contrast to several studies [8,32,33] in which DC-STAMP localization on DC was performed on cells transfected with a DC-STAMP-GFP fusion protein, we used 1A2 to localize endogenous DC-STAMP. After 8 days of culture with RANKL+M-CSF, the majority of monocytes were unable to differentiate into OC and manifested a spindle-shaped morphology (Figure 4B-a), indicative of a pre-osteoclast differentiation stage.[27] DC-STAMP protein localized intracellularly with a punctuate distribution in these cells (Figure 4B-a). In contrast, DC-STAMP protein could not be identified (Figure 4B-b, DC-STAMP: green; actin: red; nuclear: blue) in multinucleated OC from the same cultures. These polykaryons lacked DC-STAMP proteins, but displayed prominent actin rings, a structure associated with bone-resorbing capacity of OC.[28] Collectively, the FACS (Figure 4A) and confocal staining data (Figure 4B) suggest that DC-STAMP is down-regulated when monocytes differentiate into OC. Our real-time PCR data is in accordance with this conclusion (supplemental data: Figure S5).

The observation that the expression of DC-STAMP is down-regulated during OC differentiation (Figure 4A and 4B) raised an intriguing question: if DC-STAMP is not down-regulated during osteoclastogenesis, can OCP initiate differentiation and develop into mature OC? To answer this question, we overexpressed DC-STAMP in RAW264.7 cells rather than monocytes due to the technical challenges of human monocyte transfection. Interestingly, many multinucleated cells (≥3 nuclei per cell) were observed in cells transfected with the pCMV6-DC-STAMP plasmid within 16-hr post-transfection in the absence of RANKL (Figure 4C-c). In contrast, polykaryons were not detected in cells receiving no DNA (Figure 4C-a) or vector (Figure 4C-b) at 16 hours. Overexpression of DC-STAMP in pCMV6-DC-STAMP-transfected RAW264.7 cells was confirmed by western and flow cytometry (data not shown). The presence of multinucleated cells in DC-STAMP-transiently transfected RAW264.7 cells emphasized the role of DC-STAMP in osteoclastogenesis as a fusogen (Figure 4C-c and supplemental data Figure S4).[34]

To test whether downregulation of DC-STAMP is necessary for OC differentiation, we added RANKL to these transiently transfected RAW264.7 cells 24-hr post-transfection and examined their OC-forming potential. Non-transfected control cells were able to generate multinucleated TRAP+ cells in the presence of RANKL (Figure 4C-d). In contrast, cells transiently transfected with DC-STAMP failed to generate TRAP+ cells. Instead, they generated macrophage-like cells with many extending pseudopods (Figure 4C-f). The phenotypes of DC-STAMP-transfected cells suggest that continuous elevated expression of this molecule might inhibit osteoclatogenesis. However, the absence of TRAP+ cells in the control cell line (Figure 4C-e) raises the possibility that genes in the backbone of pCMV6 might have an adverse effect on OC formation.

Circulating DC-STAMP^{high} monocytes are the primary reservoir of human OCP

To determine whether the level of DC-STAMP surface expression on monocytes correlates with osteoclastogenesis potential, we analyzed osteoclast formation in DC-STAMP^{high} and DC-STAMP^{low} cells. Monocytes were first purified by monocyte enrichment kit (StemCell) from PBMC. We stained purified monocytes (>85% purity) with 1A2, sorted cells into DC-STAMP^{high} and DC-STAMP^{low} (Figure 5A, 1.9% highest and 1.8% lowest of total sorted monocytes, respectively), cultured them, and examined OC formation and bone resorption activities after culture.

A higher number of TRAP+ mature OC were generated from freshly-isolated DC-STAMP^{high} (162 per 10^5) compared to DC-STAMP^{low} (2 per 10^5) cells (Figure 5B). More than 90% of bone surface was eroded deeply by OC derived from freshly-isolated DC-STAMP^{high} human monocytes (Figure 5B-d), whereas cells derived from freshly-isolated

DC-STAMP^{low} human monocytes produced few, comparatively shallow erosion pits (<10%, Figure 5B-c). Together, these data showed a positive association between DC-STAMP expression, osteoclastogenic potential and bone resorption activity.

Role of DC-STAMP in signal transduction during osteoclastogenesis

It is known that ITAM- and ITIM-bearing receptors co-aggregate following extracellular ligand binding, which triggers downstream cellular signaling events. Following coaggregation, the cytoplasmic ITIMs undergo tyrosine phosphorylation and recruit SH2-containing proteins such as SHP-1[35]. Based on our previous finding that OCP arise from the CD16+ monocyte subset[3] and the positive correlation between CD16 and DC-STAMP surface expression (Figure 1A), we examined whether DC-STAMP physically interacts with CD16 and if DC-STAMP can recruit the SHP-1 protein, a property shared by other ITIM-bearing molecules such as PIR-B, LILR-B, and Ly49Q.[20,21]

To this end, we immunoprecipiated (IP) human monocyte proteins with 1A2 (lane 2, Figure 6A) or anti-CD16 antibody (lane 3, Figure 6A). IP lysates were analyzed by SDS-PAGE and immunoblotted (IB) with 1A2. Although different proteins were pulled down by 1A2 and anti-CD16 antibody, one common band corresponding to the location of DC-STAMP (~53 kDa, arrow in Figure 6A) was recognized by 1A2 from both IP lysates. The remaining common bands shared by 1A2-IP and anti-CD16-IP (lane 2 and 3 in Figure 6A) are likely to be proteins within the DC-STAMP-CD16 complex and thus can be pulled down by both antibodies. To examine the interaction between DC-STAMP and SHP-1, human monocyte proteins were IP with anti-SHP-1 antibody and IB with 1A2. The presence of DC-STAMP band (arrow in Figure 6B) suggests a physical interaction between DC-STAMP and SHP-1.

The presence of one tyrosine residue (^{407}SFYPSV^{412}) in the ITIM of the DC-STAMP tail suggested that DC-STAMP can be phosphorylated on the tyrosine residue of ITIM. Upon activation, ITIMs undergo tyrosine phosphorylation and recruit SH2-containing proteins.[35] Based on these data, we predicted that DC-STAMP is phosphorylated on its tyrosine residue and that DC-STAMP-associated SHP-1 is phosphorylated. To test these predictions, human monocyte proteins were IP by either anti-SHP-1 antibody or 1A2, followed by IB with anti-phosphotyrosine antibody 4G10. As indicated by arrows shown in Figure 6C, two bands corresponding to SHP-1 (68 kDa) and DC-STAMP (53 kDa) can be recognized by 4G10. This finding demonstrates that tyrosine residues are phosphorylated on DC-STAMP and on DC-STAMP associated SHP-1 proteins.

The blockade of osteoclastogenesis by 1A2 (Figure 1D, a–c) and the presence of phosphorylated tyrosines in DC-STAMP (Figure 6C) led us to examine the correlation between DC-STAMP phosphorylation and 1A2 stimulation. We cultured human monocytes in OC-promoting media (RANKL+M-CSF) in the absence or presence of 1A2 for 8 days, isolated proteins and IP by anti-SHP-1 antibody, followed by IB with anti-phosphotyrosine antibody 4G10 (Figure 6D-(I)). A phosphorylated SHP-1 band was noted on cells cultured without 1A2 but not in cultures that contained the antibody (compare lane 4 to lane 5 in Figure 6D-(I). The SHP-1 band was located by an arrow). These data suggest that 1A2 blocks OC formation either directly or indirectly via regulation of SHP-1 phosphorylation.

In the process of OC differentiation, signals from both RANK and ITAM-coupled receptors converge to activate phospholipase Cγ (PLC-γ).[13] We hypothesized that PLC-γ may be also modulated by DC-STAMP-mediated signaling pathways. To test this hypothesis, we compared the expression of phosphorylated PLC-γ in human monocytes cultured in the presence or absence of 1A2 in OC-promoting culture conditions (RANKL and M-CSF) at serial time points. Within 16 hrs, 1A2 induced a dramatic increase in phosphorylated PLC-γ2 levels (Figure 6D-(II)-d), which was not detected in cells cultured without 1A2 (Figure

6D-(II)-a). After 40 hrs, the percentage of phosphorylated PLC-γ2 level increased in all cells either treated with or without 1A2 (b and e in Figure 6D-(II)), although a minor difference in the percentage of phosphorylated PLC-γ2 was noted (54% vs. 40% when compared b to e in Figure 6D-(II)). After 64 hrs, the earliest time point when multinucleated cells appeared, phosphorylated PLC-γ2 were detected in the majority of cells in both 1A2-treated and untreated cells (c: 77% and f: 81% in Figure 6D-(II)). Our results show that i) the level of phosphorylated PLC-γ2 increased when monocytes were driven into OC differentiation (% of PLC-γ2 increased from a to c, and from d to f, Figure 6D-(II)); ii) binding of 1A2 to DC-STAMP induced a rapid increase in phosphorylated PLC-γ2 level at a relatively early time point in osteoclastogenesis. The addition of a mouse IgG2a isotype control did not increase the level of phosphorylated PLC-γ2 at the early time point (Figure 6D-(II), g to i).

Discussion

Blood monocytes differentiate into effector cells with distinct phenotypes. One of these cells, the OC, a uniquely polarized polykaryon with bone-resorbing activity, is directly involved in the pathogenesis of a spectrum of disorders. Identification of a specific surface marker on OC progenitors is of great importance, because it would assist in the evaluation of metabolic, inflammatory and neoplastic disorders, serve as a marker of treatment response, and potentially provide a novel therapeutic target. We selected DC-STAMP as a strong candidate for an OCP biomarker based on its surface localization and critical role in the regulation of cell-to-cell fusion during OC differentiation. In this study, we generated a DC-STAMP-specific antibody, examined the potential of DC-STAMP as a biomarker of OCP, characterized the expression of DC-STAMP during OC differentiation, identified an important motif ITIM on the cytoplasmic tail of DC-STAMP, and elucidated the involvement of DC-STAMP in signaling during osteoclastogenesis.

Collectively, our data indicate that DC-STAMP is a potential OCP marker. First, DC-STAMP had the highest expression on monocytes, the progenitor population of human OCP.[3,36] Second, monocytes with a higher surface DC-STAMP expression generated more OC and formed deeper and more numerous resorption pits *in vitro* compared to monocytes that expressed low surface DC-STAMP. Third, blockade of DC-STAMP with an anti-DC-STAMP antibody potently inhibited OC formation *in vitro*, a finding that underscores the essential role of DC-STAMP in OCP differentiation. Fourth, a positive correlation between CD16 and DC-STAMP surface expression as well as physical interaction of these two molecules indicate that CD16 and DC-STAMP may form a receptor complex. The association of DC-STAMP with CD16 is of particular relevance given that OCP arise from the CD16+ monocyte population in PsA.[3] Lastly, four distinct DC-STAMP expression patterns were observed on human PBMC. These patterns differed in PsA and controls and increased expression of DC-STAMP was associated with a higher frequency of OC formation *in vitro*. Thus it is plausible that increased DC-STAMP expression on monocytes may facilitate the identification of Ps patients at risk for arthritis.

The finding that human OCP arise from DC-STAMP^{high} monocytes contrasts with our previous findings in the murine RAW cell line where DC-STAMP^{lo} cells display the master fusogen phenotype.[25] It is well known that analysis of osteoclastogenesis is greatly influenced by the context of the culture conditions, timing and the source of myeloid cells.[25,37] Differences in the induction of monocyte fusion in murine and human cells have been previously reported.[37] Of note, we used freshly isolated monocytes in contrast to serially cultured RAW cells analyzed in the previous study. It is known that many cell surface markers, including CD16 and DC-STAMP (Figure 4A),[3,25] manifest significant dynamic alterations during culture. Another explanation for the discrepancies in the murine

and human studies is lineage heterogeneity in the sorted human cells. Multiple OC populations have been reported in murine bone marrow cells using a serial sorting procedure,[38] but this approach is not practical due to the low percentage of DC-STAMP +CD14+ monocytes in human PBMC. We plan to perform serial sorting on a larger population of human monocytes available from leukopheresis patients in the future to further address this potential technical issue.

Osteoclast formation and activation is regulated by a complex interplay of signaling mechanisms that involve protein-tyrosine phosphorylation.[39] Indeed, a number of immunoreceptors act in concert with RANKL and M-CSF to promote osteoclastogenesis,[13,14] including triggering receptor expressed in myeloid cells-2 (TREM-2) and osteoclast-associated receptor (OSCAR). Both TREM-2 and OSCAR are ITAM-bearing molecules that activate calcium signaling. Analogous to T cell activation which requires both signal 1 (TCR and MHC engagement) and signal 2 (co-stimulation molecule recognition), OC differentiation requires an early activation signal generated by RANKL/MCSF, followed by a second activation signal triggered by ligand engagement on the ITAM-bearing receptors.[12,40,41] Signaling molecules and cascades, including ITAM and ITIM adaptor molecules, comprise a collaborative network of interactions to regulate cell responses.[42] Indeed, ITIM and ITAM interactions take place at an early stage of immune regulation and OC formation.[20] The activation signals mediated through receptors that contain ITAM associated subunits are counterbalanced by inhibitory signals triggered by stimulation of ITIM adaptor molecules.

CD16 is considered as an ITAM-bearing protein due to its association with FcRγ [43,44] The presence of an ITAM on CD16 and an ITIM on DC-STAMP, the positive correlation between CD16 and DC-STAMP expression on fresh monocytes (Figure 1A), the reciprocal regulation of CD16 and DC-STAMP during osteoclastogenesis (Figure 4A and Chiu et al.,[3]), as well as protein-protein interactions between DC-STAMP and CD16 (Figure 6A), raised the possibility that motifs on CD16 and DC-STAMP deliver counterbalancing signals. It is well documented that coaggregation of ITAM- and ITIM-bearing receptors by an extracellular ligand is required to trigger ITIM-mediated inhibition of cellular signaling responses. Following coaggregation, the cytoplasmic ITIMs undergo tyrosine phosphorylation and recruit SH2-containing proteins such as SHP-1.[35]

Our data suggest that analogous to the two ITIM-bearing proteins PIRB and LILRB, the ITIM on DC-STAMP, delivers a negative signal based on the following observations. Osteoclastogenesis but not cell fusion was blocked when DC-STAMP was over-expressed in transfected RAW264.7 cells (Figure 4C). We also demonstrated a physical interaction between DC-STAMP and SHP-1 (Figure 6B). The finding that exposure of monocytes to 1A2 in the presence of RANKL and M-CSF decreased phosphorylation of SHP-1 (lane 5 in Figure 6D-(I)) but increased PLC-γ2 phosporylation (Figure 6D-(II)-d) is consistent with the inhibitory effect of DC-STAMP in signaling. Signaling molecules downstream of SHP-1 undergo dephosphorylation in a particular temporal sequence and at specific cellular locations to allow for efficient signaling. In particular, the phosphorylation status of SHP-1 directly determines its cellular localization and phosphatase activity.[45] The absence of detectable phosphorylated SHP-1 in 1A2-treated monocytes (Figure 6D-(I)) which were unable to differentiate into OC in the presence of RANKL+M-CSF (Figure 1D-b) suggests that binding of 1A2 to surface DC-STAMP might block phosphorylation of tyrosine on ITIM, and inhibit the recruitment of SHP-1 to DC-STAMP and its subsequent phosphorylation. As a result, the binding of 1A2 to DC- STAMP blocks inhibitory signaling delivered by ITIM on DC-STAMP, thus activation signals from ITAM-bearing molecules are relatively strengthened, which causes an increase in the level of phosphorylated PLC-γ2. Although an elevated PLC-γ2 level may favor osteoclastogenesis, monocytes fail to form

OC in the presence of 1A2 due to the inhibition of cell-to-cell fusion and a possible alteration of downstream calcium oscillations, critical for the later stages of OC differentiation. [37,46,47] An alternative explanation for the increased PLC-γ2 level is that DC-STAMP, an ITIM-bearing molecule, acts as a positive regulator of osteoclastogenesis. Parallel to the observations with the NK receptor Ly49Q,[21] DC-STAMP may compete with other ITIM-bearing receptors for SHP-1 and thus limit recruitment of SHP-1 to inhibitory ITIM-bearing proteins such as PIR-B.[21]

Based on our results and two models previously proposed by Humphrey et al.,[14] and Nimmerjahn & Ravetch,[40,41] we proposed a modifed view of the OC signaling cascades that takes DC-STAMP and CD16 into consideration as shown in Figure 7. Following activation, the ITAM in the cytoplasmic domain of CD16 is phosphorylated by a Src family kinase, that facilitates docking to SH2 sites and activation of Syk kinases, and in turn triggers Ras kinase pathway signaling through Sos. Ligand induction also triggers inhibitory signaling by the ITIM motif on DC-STAMP which attenuates Ras activation by recruitment of the SH2-domain containing phosphatase (SHP-1).[48] Factors that may activate CD16 are shown in the top box but the ligand of DC-STAMP has not been identified. Of note, our simplified model does not include all ITAM- and ITIM bearing molecules involved in osteoclastogenesis. ITAM-bearing molecules such as TREM-2 and OSCAR[18],[14] and ITIM-bearing molecules such as LILRB & PIR-B[20] must be considered as well given their important actions during osteoclast formation.

A comprehensive model of signaling that includes DC-STAMP must incorporate the findings that both DC-STAMP mRNA and protein levels fall rapidly in monocytes following exposure to RANKL. One potential explanation is that DC-STAMP expression is required to initiate the regulation of cell fusion but removal of the inhibitory signal mediated by the ITIM and SHP-1 on later stage ITAM mediated calcium signaling is also required for the OC differentiation program to fully progress. In this paradigm, temporal and spatial (migration from cell surface to cytoplasm) regulation of DC-STAMP is required for OC formation. Of note, treatment of monocytes with TNFα alone can promote polykaryon formation in a subset of monocytes.[37] In addition, TNFα triggered a rise in DC-STAMP mRNA on day 6 after TNFα exposure. Experiments are underway to better understand the interactive effect of RANKL and TNFα on DC-STAMP kinetics and function.

In conclusion, we developed a novel anti-DC-STAMP monoclonal antibody 1A2 to characterize DC-STAMP expression on human PBMC. DC-STAMP is primarily expressed on the surface of monocytes and a subset of CD3+ cells and expression levels on monocytes correlated with the level of osteoclastogenesis *in vitro.* Moreover, PBMC isolated from a subset of subjects with PsA expressed significantly higher levels of DC-STAMP by flow cytometry than controls and these findings raise the possibility that DC-STAMP is a marker for OCP in inflammatory arthritis. The declining surface expression of DC-STAMP contrasts directly with the gradual increase of CD16 expression observed during osteoclastogenesis[49]. In addition, the interaction of DC-STAMP with CD16 coupled with the identification of an ITIM in the cytoplasmic tail of DC-STAMP that binds SHP-1 provides new insights into the molecular mechanisms that underlie OC formation. Lastly, inhibition of osteoclastogenesis by 1A2 supports the concept that DC-STAMP is a potential therapeutic target for the treatment of inflammatory bone disorders.

Supplementary Material

Refer to Web version on PubMed Central for supplementary material.

Acknowledgments

All funding sources: This work was supported by the National Psoriasis Foundation (NPF) to CTR; NIH NIAID P01 AI078907, and NIH NIAMS R01 AR056702 to EMS.

References

1. Schwarz EM, Looney RJ, Drissi MH, O'Keefe RJ, Boyce BF, Xing L, Ritchlin CT. Autoimmunity and bone. Ann N Y Acad Sci. 2006; 1068:275–83. [PubMed: 16831928]
2. Ritchlin CT, Haas-Smith SA, Li P, Hicks DG, Schwarz EM. Mechanisms of TNF-alpha- and RANKL-mediated osteoclastogenesis and bone resorption in psoriatic arthritis. J Clin Invest. 2003; 111(6):821–31. [PubMed: 12639988]
3. Chiu YG, Shao T, Feng C, Mensah KA, Thullen M, Schwarz EM, Ritchlin CT. CD16 (FcRgammaIII) as a potential marker of osteoclast precursors in psoriatic arthritis. Arthritis Res Ther. 12(1):R14. [PubMed: 20102624]
4. Kukita T, Wada N, Kukita A, Kakimoto T, Sandra F, Toh K, Nagata K, Iijima T, Horiuchi M, Matsusaki H, Hieshima K, Yoshie O, Nomiyama H. RANKL-induced DC-STAMP is essential for osteoclastogenesis. J Exp Med. 2004; 200(7):941–6. [PubMed: 15452179]
5. Staege H, Brauchlin A, Schoedon G, Schaffner A. Two novel genes FIND and LIND differentially expressed in deactivated and Listeria-infected human macrophages. Immunogenetics. 2001; 53(2): 105–13. [PubMed: 11345586]
6. Yagi M, Miyamoto T, Toyama Y, Suda T. Role of DC-STAMP in cellular fusion of osteoclasts and macrophage giant cells. J Bone Miner Metab. 2006; 24(5):355–8. [PubMed: 16937266]
7. Yagi M, Miyamoto T, Sawatani Y, Iwamoto K, Hosogane N, Fujita N, Morita K, Ninomiya K, Suzuki T, Miyamoto K, Oike Y, Takeya M, Toyama Y, Suda T. DC-STAMP is essential for cell-cell fusion in osteoclasts and foreign body giant cells. J Exp Med. 2005; 202(3):345–51. [PubMed: 16061724]
8. Sawatani Y, Miyamoto T, Nagai S, Maruya M, Imai J, Miyamoto K, Fujita N, Ninomiya K, Suzuki T, Iwasaki R, Toyama Y, Shinohara M, Koyasu S, Suda T. The role of DC-STAMP in maintenance of immune tolerance through regulation of dendritic cell function. Int Immunol. 2008; 20(10):1259–68. [PubMed: 18653699]
9. Eleveld-Trancikova D, Janssen RA, Hendriks IA, Looman MW, Moulin V, Jansen BJ, Jansen JH, Figdor CG, Adema GJ. The DC-derived protein DC-STAMP influences differentiation of myeloid cells. Leukemia. 2008; 22(2):455–9. [PubMed: 17713547]
10. Sawatani Y, Miyamoto T, Nagai S, Maruya M, Imai J, Miyamoto K, Fujita N, Ninomiya K, Suzuki T, Iwasaki R, Toyama Y, Shinohara M, Koyasu S, Suda T. The role of DC-STAMP in maintenance of immune tolerance through regulation of dendritic cell function. Int Immunol. 2008
11. Iwasaki R, Ninomiya K, Miyamoto K, Suzuki T, Sato Y, Kawana H, Nakagawa T, Suda T, Miyamoto T. Cell fusion in osteoclasts plays a critical role in controlling bone mass and osteoblastic activity. Biochem Biophys Res Commun. 2008; 377(3):899–904. [PubMed: 18952053]
12. Nakashima T, Takayanagi H. Osteoimmunology: crosstalk between the immune and bone systems. J Clin Immunol. 2009; 29(5):555–67. [PubMed: 19585227]
13. Negishi-Koga T, Takayanagi H. Ca2+-NFATc1 signaling is an essential axis of osteoclast differentiation. Immunol Rev. 2009; 231(1):241–56. [PubMed: 19754901]
14. Humphrey MB, Lanier LL, Nakamura MC. Role of ITAM-containing adapter proteins and their receptors in the immune system and bone. Immunol Rev. 2005; 208:50–65. [PubMed: 16313340]
15. Blank U, Launay P, Benhamou M, Monteiro RC. Inhibitory ITAMs as novel regulators of immunity. Immunol Rev. 2009; 232(1):59–71. [PubMed: 19909356]
16. Pinheiro da Silva F, Aloulou M, Benhamou M, Monteiro RC. Inhibitory ITAMs: a matter of life and death. Trends Immunol. 2008; 29(8):366–73. [PubMed: 18602341]
17. Ivashkiv LB. Cross-regulation of signaling by ITAM-associated receptors. Nat Immunol. 2009; 10(4):340–7. [PubMed: 19295630]

18. Humphrey MB, Daws MR, Spusta SC, Niemi EC, Torchia JA, Lanier LL, Seaman WE, Nakamura MC. TREM2, a DAP12-associated receptor, regulates osteoclast differentiation and function. J Bone Miner Res. 2006; 21(2):237–45. [PubMed: 16418779]
19. Koga T, Inui M, Inoue K, Kim S, Suematsu A, Kobayashi E, Iwata T, Ohnishi H, Matozaki T, Kodama T, Taniguchi T, Takayanagi H, Takai T. Costimulatory signals mediated by the ITAM motif cooperate with RANKL for bone homeostasis. Nature. 2004; 428(6984):758–63. [PubMed: 15085135]
20. Mori Y, Tsuji S, Inui M, Sakamoto Y, Endo S, Ito Y, Fujimura S, Koga T, Nakamura A, Takayanagi H, Itoi E, Takai T. Inhibitory immunoglobulin-like receptors LILRB and PIR-B negatively regulate osteoclast development. J Immunol. 2008; 181(7):4742–51. [PubMed: 18802077]
21. Hayashi M, Nakashima T, Kodama T, Makrigiannis AP, Toyama-Sorimachi N, Takayanagi H. Ly49Q, an ITIM-bearing NK receptor, positively regulates osteoclast differentiation. Biochem Biophys Res Commun. 393(3):432–8. [PubMed: 20153723]
22. Umeda S, Beamer WG, Takagi K, Naito M, Hayashi S, Yonemitsu H, Yi T, Shultz LD. Deficiency of SHP-1 protein-tyrosine phosphatase activity results in heightened osteoclast function and decreased bone density. Am J Pathol. 1999; 155(1):223–33. [PubMed: 10393854]
23. Aoki K, Didomenico E, Sims NA, Mukhopadhyay K, Neff L, Houghton A, Amling M, Levy JB, Horne WC, Baron R. The tyrosine phosphatase SHP-1 is a negative regulator of osteoclastogenesis and osteoclast resorbing activity: increased resorption and osteopenia in me(v)/me(v) mutant mice. Bone. 1999; 25 (3):261–7. [PubMed: 10495129]
24. Moll JM, Wright V. Psoriatic arthritis. Semin Arthritis Rheum. 1973; 3(1):55–78. [PubMed: 4581554]
25. Mensah KA, Ritchlin CT, Schwarz EM. RANKL induces heterogeneous DC-STAMP(lo) and DC-STAMP(hi) osteoclast precursors of which the DC-STAMP(lo) precursors are the master fusogens. J Cell Physiol. 223(1):76–83. [PubMed: 20039274]
26. Sandor M, Hagen M, de Andres B, Lynch RG. Developmentally regulated Fc gamma receptor expression in lymphopoiesis Fc gammaR III (CD16) provides an ITAM motif for pro-T and pro-B-cells. Immunol Lett. 1996; 54(2–3):123–7. [PubMed: 9052866]
27. Coggeshall KM, Nakamura K, Phee H. How do inhibitory phosphatases work? Mol Immunol. 2002; 39(9):521–9. [PubMed: 12431385]
28. Tamir I, Dal Porto JM, Cambier JC. Cytoplasmic protein tyrosine phosphatases SHP-1 and SHP-2: regulators of B cell signal transduction. Curr Opin Immunol. 2000; 12(3):307–15. [PubMed: 10781410]
29. Borges L, Cosman D. LIRs/ILTs/MIRs, inhibitory and stimulatory Ig-superfamily receptors expressed in myeloid and lymphoid cells. Cytokine Growth Factor Rev. 2000; 11(3):209–17. [PubMed: 10817964]
30. Helming L, Tomasello E, Kyriakides TR, Martinez FO, Takai T, Gordon S, Vivier E. Essential role of DAP12 signaling in macrophage programming into a fusion-competent state. Sci Signal. 2008; 1(43):ra11. [PubMed: 18957693]
31. Lee LF, Xu B, Michie SA, Beilhack GF, Warganich T, Turley S, McDevitt HO. The role of TNF-alpha in the pathogenesis of type 1 diabetes in the nonobese diabetic mouse: analysis of dendritic cell maturation. Proc Natl Acad Sci U S A. 2005; 102(44):15995–6000. [PubMed: 16247001]
32. Eleveld-Trancikova D, Triantis V, Moulin V, Looman MW, Wijers M, Fransen JA, Lemckert AA, Havenga MJ, Figdor CG, Janssen RA, Adema GJ. The dendritic cell-derived protein DC-STAMP is highly conserved and localizes to the endoplasmic reticulum. J Leukoc Biol. 2005; 77(3):337–43. [PubMed: 15601667]
33. Jansen BJ, Eleveld-Trancikova D, Sanecka A, van Hout-Kuijer M, Hendriks IA, Looman MG, Leusen JH, Adema GJ. OS9 interacts with DC-STAMP and modulates its intracellular localization in response to TLR ligation. Mol Immunol. 2009; 46 (4):505–15. [PubMed: 18952287]
34. Vignery A. Macrophage fusion: the making of osteoclasts and giant cells. J Exp Med. 2005; 202(3):337–40. [PubMed: 16061722]

35. Huang ZY, Hunter S, Kim MK, Indik ZK, Schreiber AD. The effect of phosphatases SHP-1 and SHIP-1 on signaling by the ITIM- and ITAM-containing Fcgamma receptors FcgammaRIIB and FcgammaRIIA. J Leukoc Biol. 2003; 73(6):823–9. [PubMed: 12773515]
36. Komano Y, Nanki T, Hayashida K, Taniguchi K, Miyasaka N. Identification of a human peripheral blood monocyte subset that differentiates into osteoclasts. Arthritis Res Ther. 2006; 8(5):R152. [PubMed: 16987426]
37. Yarilina A, Xu K, Chen J, Ivashkiv LB. TNF activates calcium-nuclear factor of activated T cells (NFAT)c1 signaling pathways in human macrophages. Proc Natl Acad Sci U S A. 108(4):1573–8. [PubMed: 21220349]
38. Jacquin C, Gran DE, Lee SK, Lorenzo JA, Aguila HL. Identification of multiple osteoclast precursor populations in murine bone marrow. J Bone Miner Res. 2006; 21(1):67–77. [PubMed: 16355275]
39. Asagiri M, Takayanagi H. The molecular understanding of osteoclast differentiation. Bone. 2007; 40(2):251–64. [PubMed: 17098490]
40. Nimmerjahn F, Ravetch JV. Fc-receptors as regulators of immunity. Adv Immunol. 2007; 96:179–204. [PubMed: 17981207]
41. Nimmerjahn F, Ravetch JV. Fcgamma receptors as regulators of immune responses. Nat Rev Immunol. 2008; 8(1):34–47. [PubMed: 18064051]
42. Levy ED, Landry CR, Michnick SW. Cell signaling. Signaling through cooperation. Science. 328(5981):983–4. [PubMed: 20489011]
43. Pinheiro da Silva F, Aloulou M, Skurnik D, Benhamou M, Andremont A, Velasco IT, Chiamolera M, Verbeek JS, Launay P, Monteiro RC. CD16 promotes Escherichia coli sepsis through an FcR gamma inhibitory pathway that prevents phagocytosis and facilitates inflammation. Nat Med. 2007; 13(11):1368–74. [PubMed: 17934470]
44. da Silva FP, Aloulou M, Benhamou M, Monteiro RC. Inhibitory ITAMs: a matter of life and death. Trends Immunol. 2008; 29(8):366–73. [PubMed: 18602341]
45. Liu Y, Kruhlak MJ, Hao JJ, Shaw S. Rapid T cell receptor-mediated SHP-1 S591 phosphorylation regulates SHP-1 cellular localization and phosphatase activity. J Leukoc Biol. 2007; 82(3):742–51. [PubMed: 17575265]
46. Hogan PG, Chen L, Nardone J, Rao A. Transcriptional regulation by calcium, calcineurin, and NFAT. Genes Dev. 2003; 17(18):2205–32. [PubMed: 12975316]
47. Dolmetsch RE, Lewis RS, Goodnow CC, Healy JI. Differential activation of transcription factors induced by Ca2+ response amplitude and duration. Nature. 1997; 386(6627):855–8. [PubMed: 9126747]
48. Takai T. Roles of Fc receptors in autoimmunity. Nat Rev Immunol. 2002; 2(8):580–92. [PubMed: 12154377]
49. Chiu YG, Shao T, Feng C, Mensah KA, Thullen M, Schwarz EM, Ritchlin CT. CD16 (FcRgammaIII) as a potential marker of osteoclast precursors in psoriatic arthritis. Arthritis research & therapy. 2010; 12(1):R14. [PubMed: 20102624]

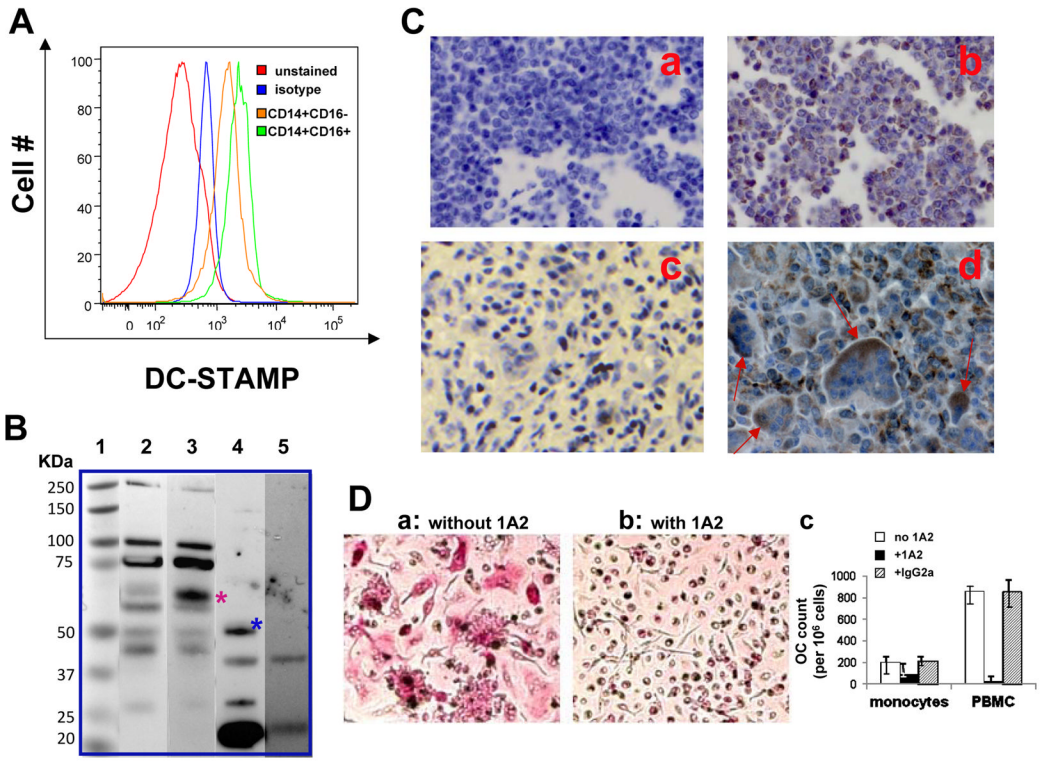

Figure 1. Functional characterization of anti-DC-STAMP mAb 1A2

(A) A positive association was noted between DC-STAMP and CD16 expression. CD14+CD16+ monocytes demonstrated a higher surface expression of DC-STAMP than CD14+CD16-cells. Human PBMC were purified by Ficoll gradient and stained with an antibody cocktail composed of 7-AAD, anti-DC-STAMP and anti-CD16 antibodies. The expression of DC-STAMP on unstained, isotype control, CD14+CD16- and CD14+CD16+ cells are labeled in red, blue, orange and green, respectively. Commercially available anti-DC-STAMP polyclonal antibody KR104 was used for this analysis. **(B)** Lane 2: total proteins isolated from the RAW cell line; lane 3: proteins isolated from a RAW cell line expressing the PTHR-DC-STAMP fusion protein; lane 4: immunoprecipitated human monocyte proteins by 1A2; lane 5: immunoprecipitated human monocyte proteins by mouse IgG2a. All proteins were denatured, separated by 10% gradient protein gel, and probed with the anti-DC-STAMP mAb 1A2 on western blots. Pink and blue asterisks label the PTHR-DC-STAMP fusion protein and DC-STAMP native protein, respectively. **(C)** DC-STAMP expression on human PBMC and multinucleated giant cells from giant cell tumor of bone was detected by immunohistochemical (IHC) staining using 1A2, (a) & (b). Human PBMC were purified by Ficoll gradient, embedded in paraffin for section, and stained with (a) mouse IgG2a isotype control, or (b) 1A2. (c) & (d). Human biopsy samples collected from giant cell tumor were sectioned, and stained with (c) mouse IgG2a isotype control, or (d) 1A2. Both 1A2 and mouse IgG2a isotype control were diluted at 1:1500 for staining. The polarized expression of DC-STAMP in the multinucleated giant cells from a giant cell tumor was labeled by arrows. **(D)** The anti-DC-STAMP mAb 1A2 was able to block OC formation in vitro. Enriched human monocytes were cultured in the absence (a) or presence (b) of 1A2 for 8 days and TRAP-stained for visualization and enumeration of OC. (c) Enriched human monocytes and PBMC isolated from different subjects were cultured in the absence (open bar), presence of 1A2 (solid bar) or with IgG2a isotype control (slash bar) for 8 days. The concentrations of 1A2 used for monocytes and PBMC were 15 μg/ml and 150 μg/ml, respectively.

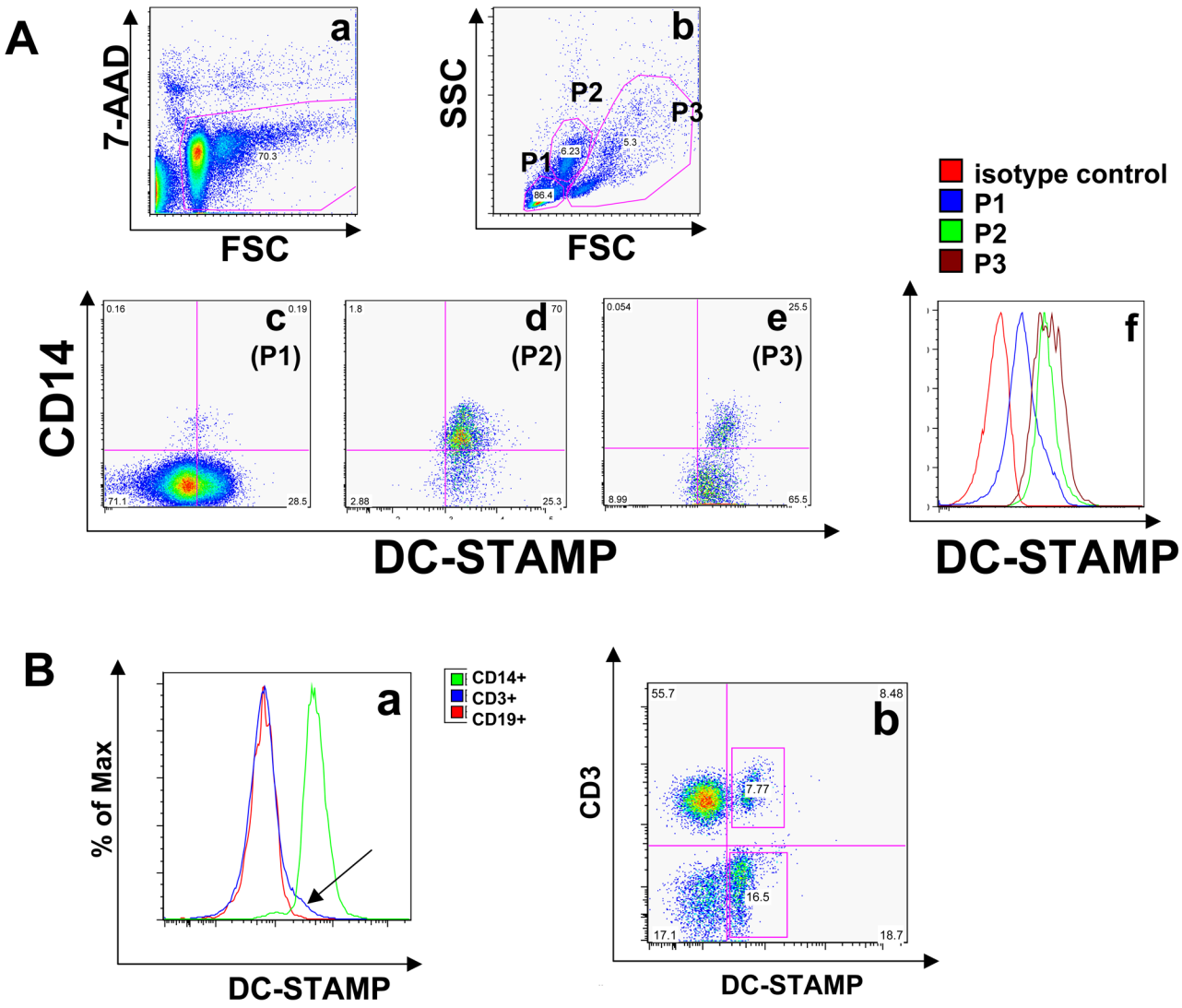

Figure 2. DC-STAMP is expressed on the surface of monocytes and a small subset of CD3+ cells on human PBMC

(A) Analysis of DC-STAMP expression on human PBMC. Human PBMC were purified from whole blood by Ficoll gradient and subjected to antibody staining and flow cytometry analysis. Human PBMC were stained with an antibody cocktail composed of 6 antibodies (see Materials and Methods for details). (a) Dead (7AAD+) cells were first excluded from our analysis; and (b) live PBMC were gated based on cell size by FSC and cell granularity by SSC into 3 cell subsets (P1, P2, and P3). The expression of CD14 and DC-STAMP on the P1, P2 and P3 subset is shown in (c), (d) and (e), respectively. (f) The surface expression of DC-STAMP in P1-(blue), P2-(green), P3-(purple) gated cells. The red line represents the isotype control. Data shown is representative of 8 subjects. **(B)** DC-STAMP is expressed on a small subset of CD3+ cells. Human PBMC were purified and stained with an antibody cocktail composed of 6 antibodies (see Materials and Methods for details). (a) Monocytes, T and B cells were identified by gating of CD14+, CD3+ and CD19+ cells, respectively. The histogram shows the overlay of DC-STAMP expression on CD14+ (green line), CD3+ (blue line), and CD19+ (red line) populations. A small percentage of CD3+ are DC-STAMP+ (indicated by arrow). (b) The relative expression of DC-STAMP and CD3 on human PBMC. Data shown here represent staining phenotypes from 3 healthy controls.

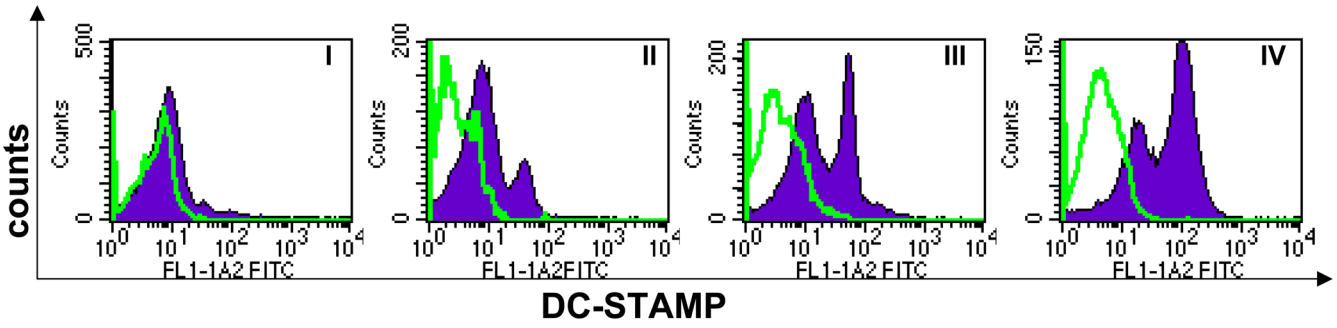

DC-STAMP pattern	I	II	III	IV
# of subjects				
healthy control	11	0	0	0
PsA patients	4	6	5	6
OC# (per 10^6 PBMC)				
median	50	98	105	203
inter-quartile range	17 - 105	21 - 390	62 - 131	35 - 340

Figure 3. Human PBMC have four distinct DC-STAMP expression patterns that differ between Ps/PsA and HC subjects

Four distinct DC-STAMP expression patterns were observed on human PBMC. PBMC were isolated from 11 healthy control (HC) and 21 PsA subjects and stained with the 1A2-FITC antibody. Dead cells were excluded by 7-ADD. Green lines represent the isotype control. The number of subjects observed in each pattern. Fisher's exact revealed significant difference among HC and PsA in 4 DC-STAMP patterns (p-value=0.01). Table 2 summarizes the definition of 4 DC-STAMP patterns and the distribution of HC and PsA patients in these 4 patterns.

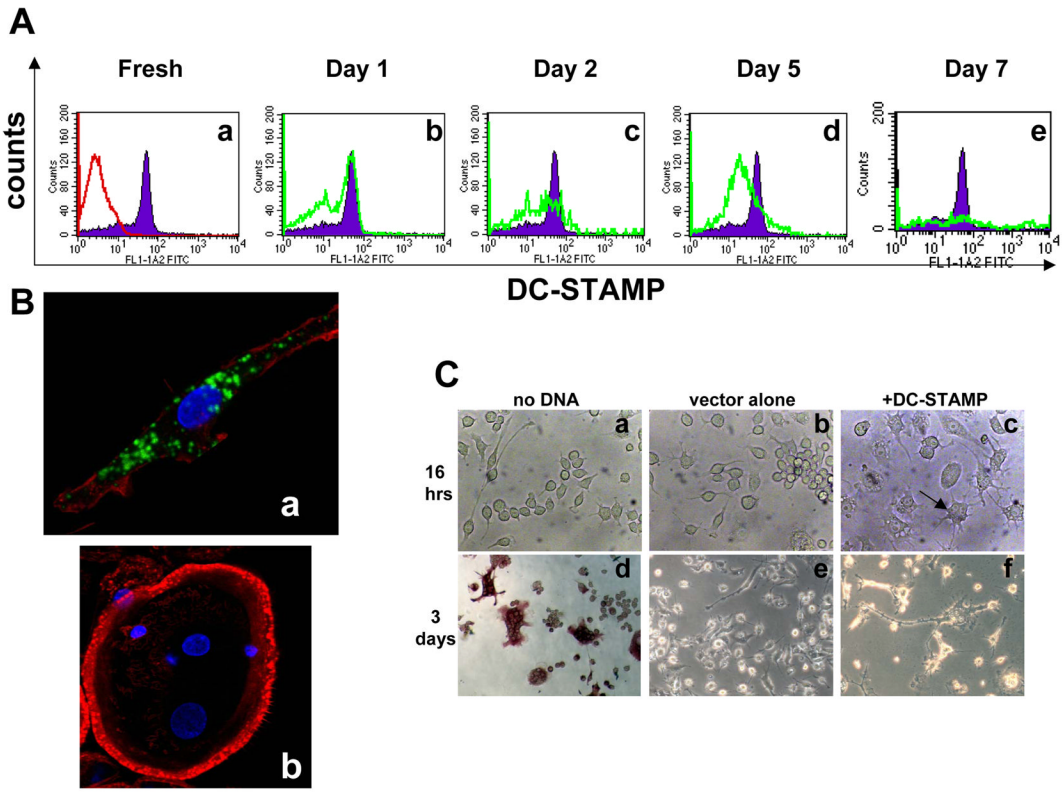

Figure 4. DC-STAMP is down-regulated in human monocytes during ostoeclastogenesis

(A) Dynamic changes of DC-STAMP surface expression on human monocytes during osteoclastogenesis. Enriched human monocytes were cultured in media supplemented with RANKL and M-CSF, and the surface expression of DC-STAMP was examined at different time points (a:day0, b:day1, c:day2, d:day5, e:day7). Purple areas in each panel represent the original DC-STAMP expression level on fresh monocytes and open green lines show the expression of DC-STAMP at the various time points. Isotype control is shown in red (a). **(B)** Cellular localization of DC-STAMP. Human monocytes were cultured with RANKL+M-CSF for 8 days, fixed and immunostained with DAPI which binds to nuclei (blue), 1A2 anti-DC-STAMP-FITC (green), and rhodamine phalloidin for actin (red). Localization of DC-STAMP on a spindle-shaped pro-OC (a) and on mature OC (b). Cells shown in (a) and (b) were cultured on a single slide with the same magnification. The images are representative of ten cells with similar phenotypes (mononuclear vs. multi-nucleated, and spindle-shaped vs. large round shape). **(C)** Overexpression of DC-STAMP on RAW 264.7 cells. RAW 264.7 cells were left untransfected (a), transfected with the pCMV6-entry vector (b), or the pCMV6-DC-STAMP (c) plasmid. (a) to (c) showed the phenotypes of cells 16-hr post-transfection. A multinucleated cell which went thru cell-to-cell fusion more than once as evidenced by the presence of 4 nuclei was labeled by an arrow in (c). RANKL was added to the cultures 24-hr post-transfection to promote OC formation. The phenotypes of cells after 3 days in culture were shown from (d) to (f).

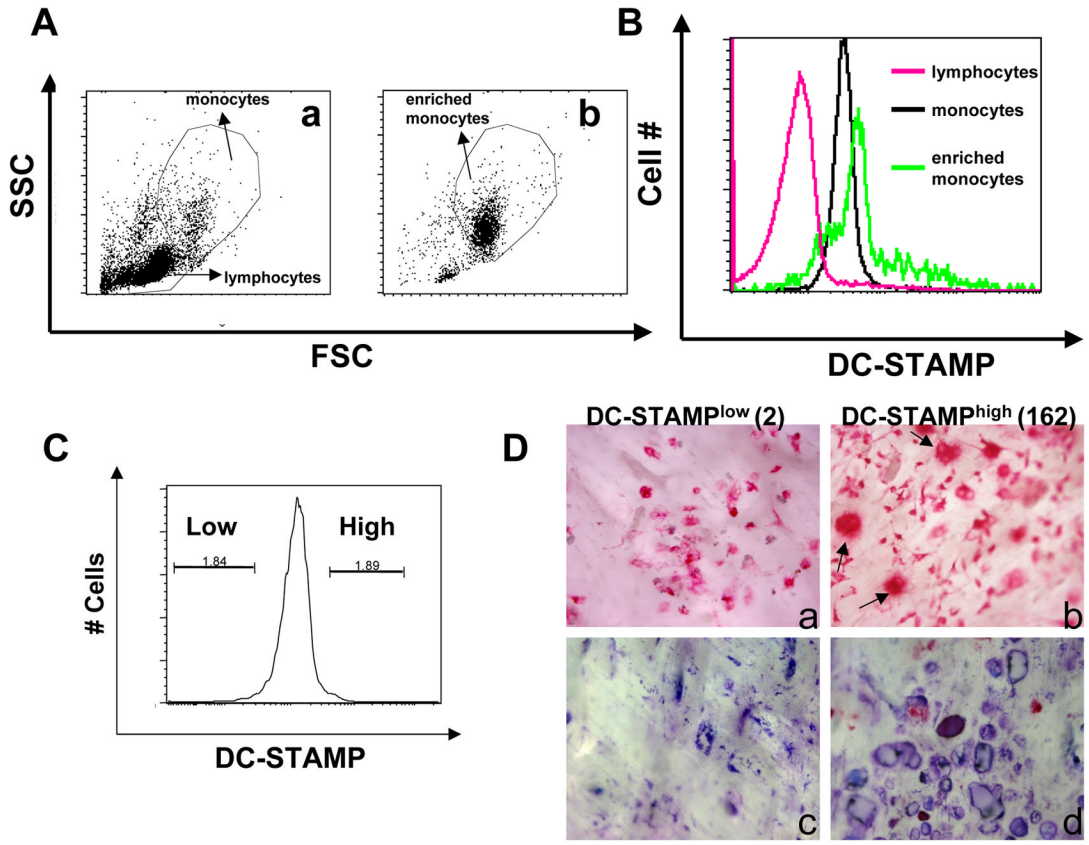

Figure 5. Human DC-STAMP^{high} cells demonstrate a higher osteoclastogenesis potential

(A) Human monocytes were negatively selected and enriched by resetting (StemCell). (a) human PBMC before enrichment; (b) human PBMC after enrichment. **(B)** DC-STAMP expression levels on enriched monocytes ((A)-b), monocytes before enrichment, and lymphocyte ((A)-a). **(C)** Gating strategy of human monocytes based on the DC-STAMP expression. Human monocytes were first enriched by a monocyte enrichment kit (StemCell), stained with 1A2-FITC and 7-AAD. Live monocytes (7-AAD negative) were gated as shown in Figure 5(A)-b and sorted into DC-STAMP^{high} and DC-STAMP^{low} (1.9% and 1.8% of the highest and lowest). **(D)** Bone resorption activity of DC-STAMP^{high} and DC-STAMP^{low} cells. Sorted DC-STAMP^{high} and DC-STAMP^{low} cells shown in (A) were cultured with bone wafers for 14 days in the presence of RANKL and M-CSF. Numbers in parentheses represent the total number of TRAP+ OC per 10^5 sorted cells. OC and erosion pits on bone wafers by DC-STAMP^{low} and DC-STAMP^{high} cells were shown in (a & b) and (c & d), respectively. Representative of three individual experiments performed on HC.

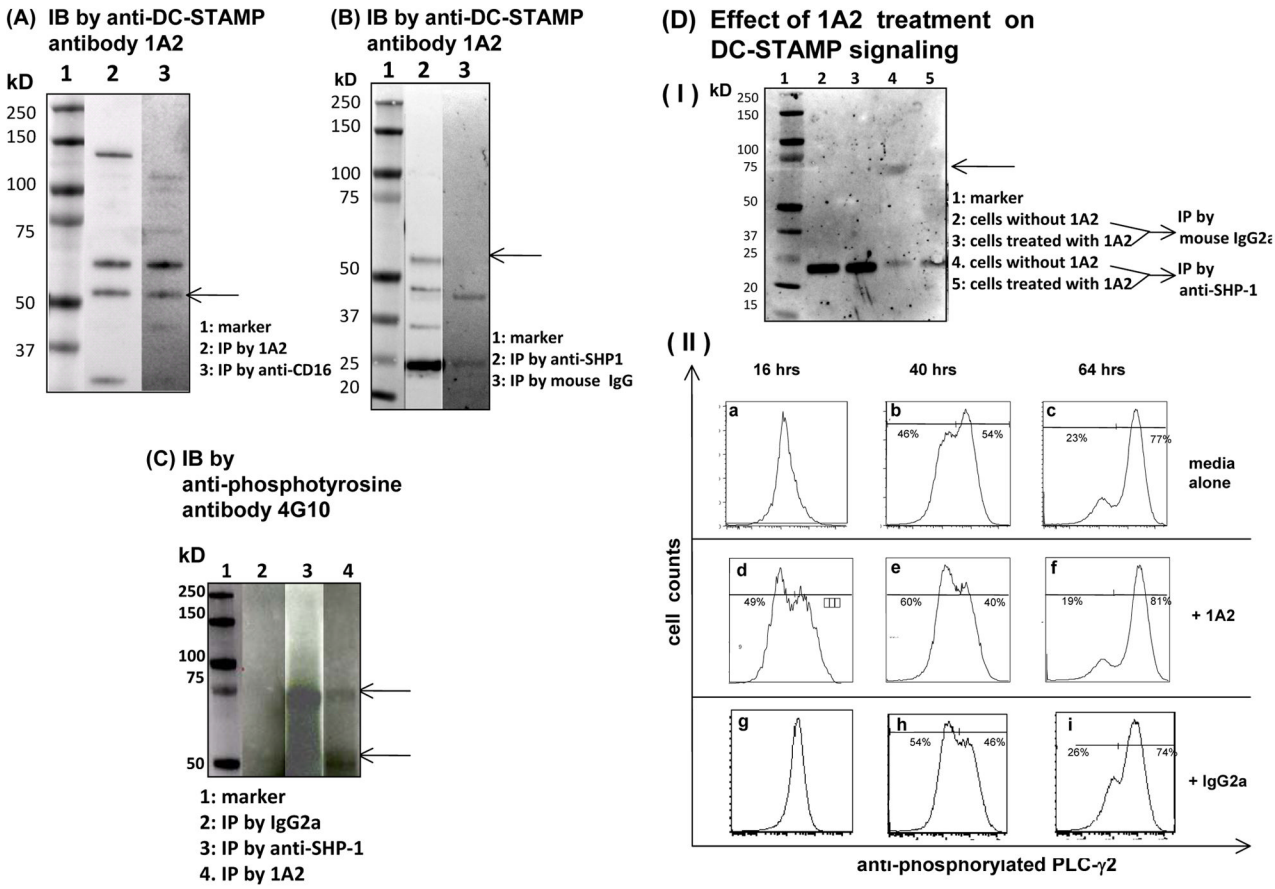

Figure 6. DC-STAMP proteins are phosphorylated on tyrosine residues, interact with SHP-1 and CD16, and may be involved in signal transduction

(A) Proteins were isolated from fresh human monocytes, immunoprecipitated (IP) with anti-DC-STAMP antibody 1A2 (lane 2) or with anti-CD16 antibody (lane 3). IP lysates were analyzed by SDS-PAGE followed by immunoblotting (IB) with 1A2. Arrow shows the DC-STAMP band (~53 kDa). **(B)** Proteins were isolated from fresh human monocytes, IP with anti-SHP1 antibody (lane 2) or with the control antibody mouse IgG (lane 3). IP lysates were analyzed by SDS-PAGE followed by IB with 1A2. Arrow shows the DC-STAMP band (~53 kDa). **(C)** Proteins were isolated from fresh human monocytes, IP with mouse IgG2a (lane 2), or anti-SHP1 antibody (lane3) or anti-DC-STAMP antibody 1A2 (lane 4). IP lysates were analyzed by SDS-PAGE followed by IB with anti-phosphotyrosine antibody 4G10. The bands of SHP-1 (~70 kDa) and DC-STAMP (~53 kDa) are marked by arrows. **(D)** Examination of 1A2 effects on DC-STAMP signaling. **(I)** Human monocytes were cultured in OC-promoting media (RANKL+M-CSF) in the absence (lanes 2 and 4) or presence (lanes 3 and 5) of 1A2 for 8 days. Proteins were isolated and IP with mouse IgG2a (lanes 2 and 3) or with anti-SHP-1 antibody (lanes 4 and 5), and subjected to SDS-PAGE, followed by IB with anti-phosphotyrosine antibody 4G10. Arrow indicates the location of the SHP-1 band. **(II)** Purified human monocytes were cultured in OC-promoting media (RANKL+M-CSF) in the absence (a to c) or the presence of 1A2 (d to f), or in the presence of mouse IgG2a isotype control (g to i). Cells were harvested and analyzed at 3 different time points (16hrs: a &d; 40 hrs: b & e; 64 hrs: c & f) for phosphorylated PLC-γ2 expression by intracellular staining with the anti- PLC- γ2 antibody (pY759) and flow cytometric analysis.

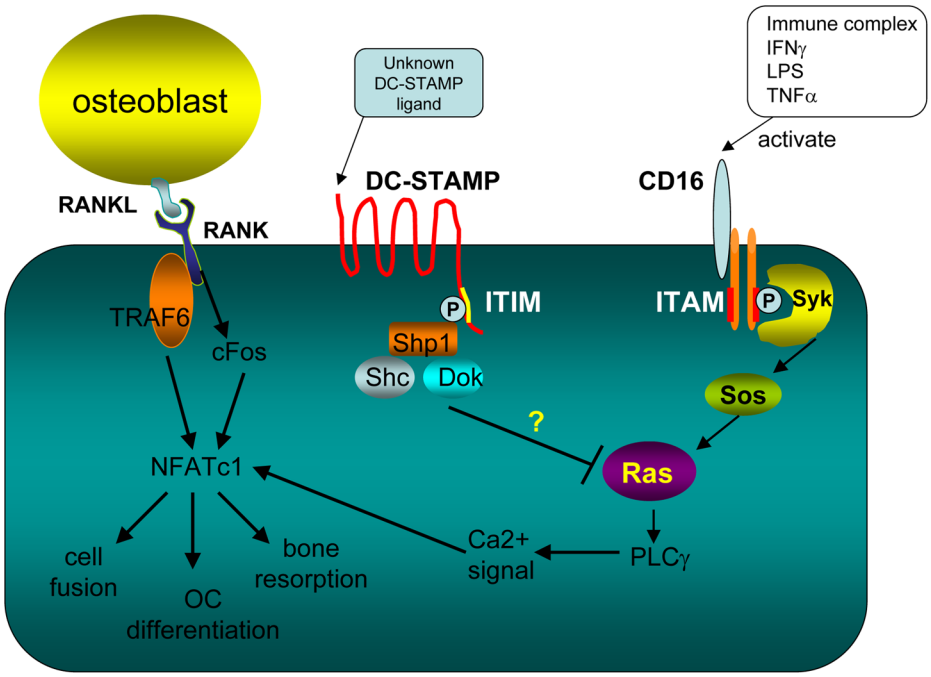

Figure 7. A model of signaling cascades induced by DC-STAMP, CD16, and RANK during osteoclast differentiation

This diagram is a modification of several models previously proposed by Humphrey et al.,[14] Nimmerjahn & Ravetch,[40,41] and Nakashima & Takayanagi.[12] Briefly, DC-STAMP and CD16 are activated after ligand binding, which triggers the phosphorylation of ITIM and ITAM to recruit SHP-1 and Syk, respectively. The balance (net readout) between the activation and inhibitory signals delivered from ITAM and ITIM will determine if downstream osteoclastogenic genes will be activated through PLC-γ and Ca^{2+}-NFATc1 regulation. CD16 and DC-STAMP were selected as the representatives of ITAM- and ITIM-bearing molecules in this figure. However, other ITAM- (OSCAR and TREM-2) and ITIM- (LILRB, PIRB and Ly49Q) bearing molecules also modulate calcium signaling through PLCγ. A more detailed explanation of this model can be found in the “Discussion”.

Table 1

The anti-DC-STAMP mAb 1A2 had an inhibitory effect on OC formation.

Subject[a]	without 1A2[b]	with 1A2[b, c]
A	125	0
B	740	0
C	500	15
D	155	80
E	745	0
F	670	270

[a] HC, Ps or PsA patients

[b] numbers of OC derived from 10^6 CD14+ cells

[c] constant presence of 1A2 in the culture at the concentration of 15 μg/ml.

Table 2

Classification of four major DC-STAMP patterns in human PBMC.

DC-STAMP pattern	DC-STAMP+/− ratio* X 100	Number of Subject	
		HC	PsA
I	1 to 20	11	4
II	20 to 67	0	6
III	68 to 240	0	5
IV	> 240.0	0	6

* the percentage of DC-STAMP+ cells in total human PBMC is divided by that of DC-STAMP- cells.